ISSN 2075-1133, Inorganic Materials: Applied Research, 2022, Vol. 13, No. 2, pp. 531–535. © Pleiades Publishing, Ltd., 2022.
Russian Text © The Author(s), 2021, published in Perspektivnye Materialy, 2021, No. 8, pp. 74–80.

Aspects of Pore Filling in Synthesis of FeNi Alloy Nanowires Using Track-Etched Membranes

I. M. Doludenko[a,b]

[a] *National Research University Higher School of Economics, Moscow, 101000 Russia*
[b] *Federal Scientific Research Centre Crystallography and Photonics, Russian Academy of Sciences, Moscow, 119333 Russia*
e-mail: doludenko.i@yandex.ru

Received January 27, 2021; revised February 17, 2021; accepted February 18, 2021

Abstract—Fe–Ni alloy nanowires (NWs) with the elemental composition similar to permalloy (20 wt % iron and 80 wt % Ni) are prepared by template-assisted synthesis using track-etched polyethylene terephthalate membranes (pore diameter of 100 nm) as the template. To obtain a solid contact at the pore bottom, the template matrix is specially prepared for electrodeposition of the metals into its pores. The NW growth kinetics is studied, and the dependence of NW length on the deposition time is established. The morphology and geometry of synthesized NWs is studied by scanning electron microscopy. The NW growth rate is shown to change at different stages of matrix pore filling and vary nonlinearly. The current efficiency is calculated at the different stages of matrix filling, and changes in this parameter correlate with the variation of growth rate. Possible explanations of the nonlinear behavior of growth rate are provided. The dependence of average NW length on deposition time is described by an equation obtained by the method of linear interpolation.

Keywords: template synthesis, track-etched membranes, electrodeposition, nanowires, growth kinetics
DOI: 10.1134/S2075113322020125

INTRODUCTION

Currently, there is a considerable interest in developing new methods for synthesis of different types of nanostructures and studying their structural aspects and properties. One-dimensional nanostructures such as nanowires (NWs), nanorods, and nanothreads display a set of unique properties [1–3]. Template-assisted (matrix) synthesis is a common method for preparation of such structures [4]. Essentially, in this method, regular-shaped pores, which are through holes in a special-purpose matrix, are filled with material of interest. Porous aluminum oxide (PAO) [5] and track-etched membranes (TMs) [6] are frequently used as the matrix. These two types of matrices have different properties. As an example, PAO can be prepared with a high pore density, but the possibility to simultaneously manipulate the pore diameter and pore density is quite limited. Further, attempts to fabricate PAO matrices with strictly cylindrical pores were unsuccessful [7], which is another limitation of this material. Despite random distribution of pores in polymer TMs and their possible overlaps, unique features of these materials include flexibility and the possibility to purposely manipulate the pore shape; in addition, their pore density and diameter can be varied independently in a broad range.

In this work, we performed electrolytic deposition of iron and nickel in pores of TMs used here as templates, with the composition of electroplated material corresponding to permalloy.

NWs made of this type of structures attract interest owing to their potential use in medicine as components of electromagnetic wave transmitters and/or receivers, memristors, and flexible microelectronics, among other things.

Single-metal NWs had been fabricated already in first studies dedicated to template synthesis. For instance, cobalt and nickel replicas were obtained (probably for the first time) in pores of an oxide matrix [8], and such structures were proposed for use in high-density magnetic storage. Subsequently, techniques were developed to prepare NWs with more complex composition, i.e., so-called alloyed and layered NWs. The possibility to create such diverse structures is a unique feature of the method of electrochemical deposition [9–11].

Fe–Ni and Fe–Co NWs were compared in a number of studies. The magnetic behavior of the two types of alloys was found to depend on the ratio of alloy components and their orderliness [12]. Further, conditions required for synthesis of layered NWs were also reported. Synthesis of Fe–Co and Fe–Ni NWs was carried out in POA pores and the resulting materials were compared [13]. Distinctions between the properties of the two types of electrodeposited NWs were identified, and the effect of thermal treatment on their

structure was established. Specifically, it was revealed that coercive force H_c in the Fe–Ni NWs increases with increase in their length, whereas the opposite effect was observed for the Fe–Co NWs. Annealing did not affect the magnetic behavior of Fe–Ni samples, whereas a considerable increase in coercive force was detected in Fe–Co samples. We note that POA was used as the template matrix in the overwhelming majority of published studies. With TMs, however, there is an additional possibility to manipulate the pore shape and size and create components for flexible electronics. FeCo and FeNi NW arrays synthesized in pores of polyethylene terephthalate matrices were studied in [14–16]. Growth patterns observed in deposition using a two-electrode configuration were established along with the influence of pore diameter. In the studies cited, Mössbauer spectroscopy was used to reveal the orientation of the magnetization vector within the NW arrays, and, in particular, in samples with pores of small diameter, the magnetization vector was found to be oriented along the NW axis. With increase in the pore diameter and/or decrease in the deposition voltage, the parameters of Mössbauer spectra of resulting samples were fairly similar to those of corresponding bulk materials. The same method was used for indirect determination of NW metal content. Studies of the magnetic properties of NW showed that H_c and remanence increased in response to a decrease in the pore diameter or an increase in NW growth rate. The effect of anomalous codeposition of iron was revealed in [17], and it was further shown that the ratio of constituent metals in NWs may vary lengthwise. These problems, however, were not addressed in detail in the cited study.

The literature survey showed that, in particular, the issue with rigorous control of pore filling in TMs and filling kinetics has been little studied.

The aim of this work was to study the NW growth rate and current efficiency at different stages of matrix template filling. This study will make it possible to fabricate NWs with precise dimensions.

EXPERIMENTAL

NWs studied in this work were prepared using commercial polymer matrices, i.e., TMs ("nuclear filters"), with through pores with cylindrical cross sections (Joint Institute for Nuclear Research, Dubna, Russia) and the following specifications: pore diameter, 100 nm; filter thickness, 12 μm; and pore density, $\approx 1.2 \times 10^9$ cm^{-2}. An electrically conducting layer on the membrane surface was created by plating a metallic layer in two stages. At the first stage, a thin amorphous copper sublayer (50 nm) was created by thermal sputtering in vacuum using a VUP-4 unit, with the layer not closing pores of the polymer matrix. To close the pores completely and create a continuous, solid contact layer, a copper layer with a thickness of 4–5 μm was electroplated galvanostatically onto the sputtered sublayer by applying a current density of 71 A/cm^2 for 30 min.

NWs were created by electrodeposition into pores of a template matrix using a plating bath composed of $NiSO_4 \cdot 7H_2O$ (16 g/L), $NiCl_2 \cdot 6H_2O$ (40 g/L), and $FeSO_4 \cdot 7H_2O$ (8 g/L). Similarly, the following additives to the bath were used: boric acid (H_3BO_3, 25 g/L; to maintain pH 2.4), sodium lauryl sulfate (1 g/L; to improve wettability of matrix pores), and ascorbic acid (1 g/L; to prevent ferrous ions from oxidation to ferric ions).

The process was carried out in a dedicated cell. The surface area of a TM involved in electrodeposition was 1.8 cm^2, and thus the area of working electrode, i.e., the surface area of matrix pores, was 0.17 cm^2. Electrodeposition was performed in the potentiostatic mode at a potential of 1.5 V using an iron anode and an Elins P-2X potentiostat/galvanostat to control the applied potential. In our previous work, we carried out a detailed study of the relationship between the structure of Fe–Ni and Fe–Co nanowires and the electrodeposition conditions such as electrolyte composition and applied potential [18]. The adopted deposition conditions enabled us to produce NWs of a Fe–Ni solid solution based on the Ni lattice with the Fe : Ni ratio of 24 : 76.

Prepared samples were studied by scanning electron microscopy (SEM) on a JSM-6000Plus instrument (JEOL) operated in the secondary electron mode at an accelerating voltage of 15 kV.

EXPERIMENTAL RESULTS AND DISCUSSION

In this study, TMs filling was carried out potentiostatically at a potential of 1.5 V using an iron anode to make up for the loss of iron ions in the electrolyte and different deposition times. Initially, a current transient (a characteristic of electrodeposition process) for the entire process was recorded to determine the time required for matrix filling (Fig. 1).

As can be seen, the process of matrix filling can be divided into five stages: (1) the onset of NW growth, when the current decreases following the Cottrell law [19]; (2) filling of matrix pores and subsequent development of a diffusion layer; (3) outgrowth of deposited metal on the surface of the matrix; (4) complete filling of the matrix; and (5) formation of a continuous metal layer on the surface of the matrix.

Two series of samples differing in the deposition time were prepared to study the kinetics of filling of matrix pores: one without overgrowth and the other with overgrowth, i.e., in the latter case, the deposited metal overfilled the pores to form "caps" on the surface of the matrix [20]. The samples were then mounted on a special holder to enable SEM characterization of their face ends. For microscopic studies, samples without overgrowths were prepared by remov-

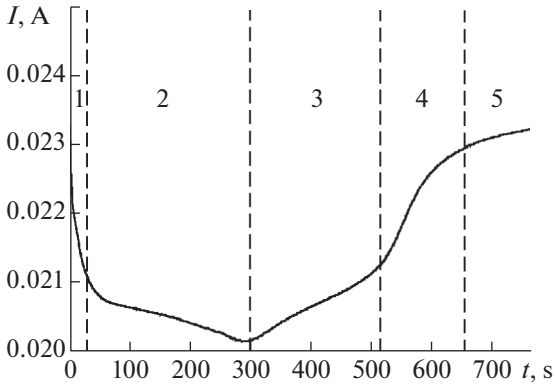

Fig. 1. Current transients characterizing the pore filling process.

ing their matrix in concentrated NaOH solution (240 g/L), while samples with overgrowth were studied from the side of their cross sections. SEM images of the samples are presented in Fig. 2.

The microscopic study of prepared samples showed that NWs essentially reproduced the shape of pores, with their diameter larger by 10–15% than that expected on the basis of the diameter of matrix pores, which is due to the oxidation of NWs in air. Since pores and, consequently, the NWs are at a small angle to the surface of the matrix, we estimated the average projection of NWs on the surface normal. Current transients were recorded during electrodeposition as characteristics the pore filling process. These data were used to calculate the charged passed, which is directly related, via the Faraday law, to the average length of deposited NWs, and thus to estimate the rate of NW growth.

Similarly, we determined the current efficiency of electrodeposition, which is the amount of charge (in %) consumed only in metal deposition and not in side reactions, using the formula

$$B_Q = \frac{\pi r^2 HNS\rho Fz}{Q_f(M_{\mathrm{Fe}}C_{\mathrm{Fe}} + M_{\mathrm{Ni}}C_{\mathrm{Ni}})},$$

where Q_f is the actual amount of charge passed (C), r is the pore radius (cm), H is the NW length (cm), N is the pore density (cm^{-2}), S is the area of the sample (cm^2), ρ is the density of material calculated from its lattice parameter ($\mathrm{g/cm}^3$), F is the Faraday constant (C/mol), z is the ion valence number, M_{Fe} and M_{Ni} are the atomic masses of the respective metals, and C_{Fe} and C_{Ni} are their mass fractions (wt %) in the deposited material.

The current efficiency was found to vary depending on the stage of the process, with its average value being 48.4%. The side reaction of hydrogen evolution is the major contributor to diminution of current efficiency. Inhomogeneous NW growth is a consequence of this process, because part of NWs are blocked by gas bubbles, which slows their growth, while NWs that are not blocked "benefit" from this situation, because their growth is promoted at the expense of slowed growth of the blocked NWs. This causes local (isolated) overgrowths to emerge when the matrix is filled to only

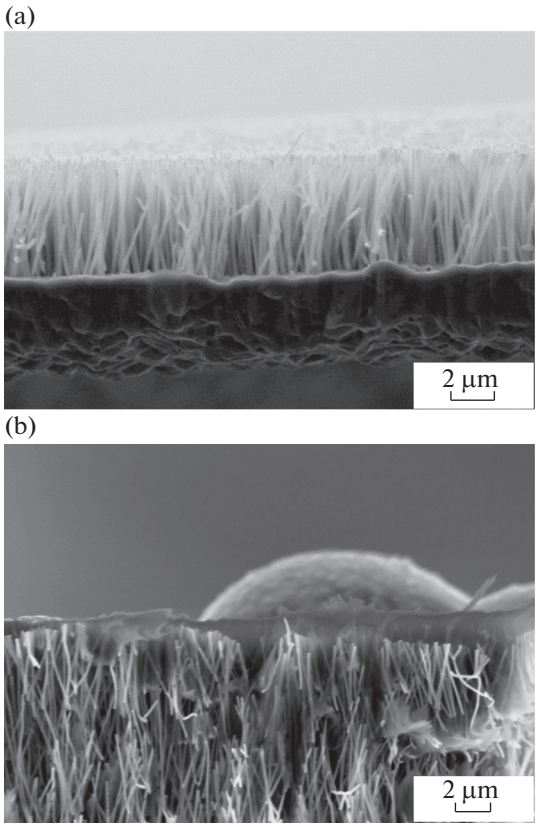

Fig. 2. SEM images of NW samples: (a) with matrix removed (growth time of 300 s) and (b) with matrix, cross-sectional view (growth time of 600 s).

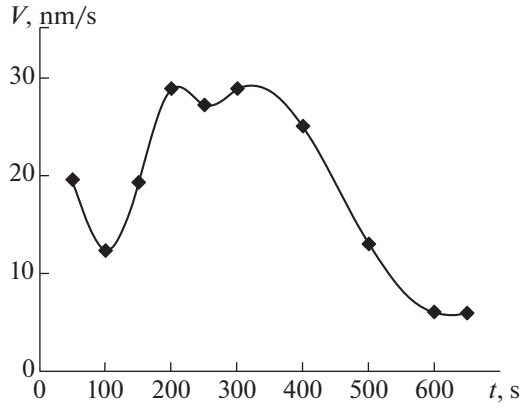

Fig. 3. Time dependence of the NW growth rate at different stages of matrix filling.

Table 1. Results of calculations of the amount of charged passed, growth rate, and current efficiency

Process characteristics	Growth time, s									
	50	100	150	200	250	300	400	500	600	650
Charge passed, C	0.8	2.1	2.6	4.1	4.3	6	7.1	9.4	11.4	12.4
NW length, μm	0.98	1.6	2.56	4	5.36	6.8	9.3	10.6	11.2	11.5
Growth rate, nm/s	19.6	12.4	19.2	28.8	27.2	28.8	25	13	6	6
Current efficiency	58.7	14	46	46.3	59.3	53.4	62.0	53.3	46.5	44

60%, with their number increasing as the process continues.

The NW length obtained from the results of SEM study and the calculated amount of charge, growth rate, and current efficiency are reported in Table 1.

The presented results imply that both the growth rate and amount of charge passed vary nonlinearly with deposition time. Changes in the current efficiency correlate with changes in the growth rate. The time dependence of the growth rate at different stages of pore filling is presented in Fig. 3 to give a visual idea of the results under discussion.

Presumably, the high growth rate observed during the first stage (0–50 s) is due to a current jump at the onset of deposition and the high concentration of electrolyte near the deposition surface. Within the time interval of 50 to 100 s, the electrolyte near the deposition surface suddenly becomes depleted. The subsequent linear increase in the growth rate (100–200 s) is related to the growth of the diffusion layer until it reaches pore openings at the matrix surface. This is followed by the formation of a common diffusion layer, which involved all pores, and the growth rate establishes and remains constant until local overgrowths emerge to form caps at the surface of the matrix. As the process continues, the deposition predominantly occurs at the caps owing to their larger surface area and the shorter distance to the anode, which causes the NW growth rate in matrix pores to diminish.

The following equation obtained by interpolation of the data presents the time dependence of average NW length before overgrowths emerge:

$$H = 4\times10^{-9}t^3 + 3\times10^{-5}t^2 + 0.0128t.$$

where t is the growth time (s) and H is the NW length (μm).

This dependence was confirmed by experiment.

CONCLUSIONS

The growth kinetics of Fe_{24}–Ni_{76} alloy NWs was studied, and key growth stages were identified.

The growth rate was found to change nonlinearly at different stages of pore filling, presumably, owing to diffusion of metal ions occurring within the confinement of pore volume, which leads to the development of a diffusion layer and ultimately establishment of a constant NW growth rate.

An equation presenting the length of growing NWs as a function of the NW deposition time was obtained on the basis of experimental data. The calculated current efficiency of NW electrodeposition was 48.4%.

FUNDING

This work was performed with partial support from the Ministry of Science and Higher Education of Russia within a state assignment to the Federal Scientific Research Centre (FSRC) Crystallography and Photonics, Russian Academy of Sciences (RAS).

Scanning electron microscopy studies were performed using the facilities of the Centre for Collective Use of FSRC Crystallography and Photonics, RAS.

CONFLICT OF INTEREST

The author declares that he has no conflicts of interest.

REFERENCES

1. Anishchik, V.M., Borisenko, V.E., Zhdanok, S.A., Tolochko, N.K., and Fedosyuk, V.M., *Nanomaterialy i nanotekhnologii (Nanomaterials and Nanotechnology)*, Borisenko, V.E. and Tolochko, N.K., Eds., Minsk: Belorus. State Univ., 2008.
2. Borisenko, V.E., Danilyuk, A.L., and Migas, D.B., *Spintronika (Spintronics)*, Moscow: Lab. Znanii, 2017.
3. Eliseev, A.A. and Lukashin, A.V., *Funktsionalnye materialy* (Functional Nanomaterials), Tret'yakov, Yu.D., Ed., Moscow: Fizmatlit, 2010.
4. Martin, C.R., Nanomaterials: A membrane-based synthetic approach, *Science*, 1994, vol. 23, no. 266, pp. 1961–1966.
5. Masuda, H. and Fukuda, K., Ordered metal nanohole arrays made by a two-step replication of honeycomb structures of anodic alumina, *Science*, 1995, vol. 268, no. 5216, pp. 1466–1468.
6. Frolov, K.V., Zagorskii, D.L., Lyubutin, I.S., et al., Synthesis, phase composition, and magnetic properties of iron nanowires prepared in the pores of polymer track-etched membranes, *JETP Lett.,* 2014, vol. 99, no. 10, pp. 570–576. https://doi.org/10.1134/S0021364014100051

7. Petukhov, D.I., Napolskii, K.S., and Eliseev, A.A., Permeability of anodic alumina membranes with branched channels, *Nanotechnology,* 2012, vol. 23, art. ID 335601.
8. Kawai, S. and Ueda, R.J., Magnetic properties of anodic oxide coatings on aluminum containing electrodeposited Co and Co–Ni, *J. Electrochem. Soc.*, 1975, vol. 122, no. 1, pp. 32–36.
9. Lupu, N., *Electrodeposited Nanowires and Their Applications*, Croatia: InTech, 2010. https://www.intechopen.com/chapters/8903
10. Vázquez, M., *Magnetic Nano- and Microwires: Design, Synthesis, Properties and Applications,* Woodhead, 2015.
11. Davydov, A.D. and Volgin, V.M., Template electrodeposition of metals. Review, *Russ. J. Electrochem.*, 2016, vol. 52, no. 9, pp. 806–831.
12. Alonso, J., Khurshid, H., Sankar, V., Nemati, Z., Phan, M.H., Garayo, E., García, J.A., and Srikanth, H., FeCo nanowires with enhanced heating powers and controllable dimensions for magnetic hyperthermia, *J. Appl. Phys.,* 2015, vol. 117, no. 17, art. ID 17D113.
13. Steven, S.-L. Zhang, Z., Zhou, Y., Li, D., Heinonen, O., Kalska-Szostko, B., Klekotka, U., and Olszewski, W., Mode coupling in spin torque oscillators, *J. Magn. Magn. Mater.*, 2019, vol. 484, pp. 227–242.
14. Zhou, S., Wang, C., Zheng, C., and Liu, Y., Manipulating skyrmions in synthetic antiferromagnetic nanowires by magnetic field gradients, *J. Magn. Magn. Mater.*, 2020, vol. 493, pp. 165740–165743.
15. Frolov, K.V., Zagorskii, D.L., Lyubutin, I.S., et al., Magnetic and structural properties of Fe–Co nanowires fabricated by matrix synthesis in the pores of track membranes, *JETP Lett.*, 2017, vol. 105, no. 5, pp. 319–326. https://doi.org/10.1134/S0021364017050083
16. Zagorskiy, D.L., Frolov, K.V., Bedin, S.A., et al., Structure and magnetic properties of nanowires of iron group metals produced by matrix synthesis, *Phys. Solid State,* 2018, vol. 60, no. 11, pp. 2115–2126. https://doi.org/10.1134/S1063783418110367
17. Frolov, K.V., Chuev, M.A., Lyubutin, I.S., Zagorskii, D.L., Bedin, S.A., Perunov, I.V., Lomov, A.A., Artemov, V.V., Khmelenin, D.N., Sulyanov, S.N., and Doludenko, I.M., Structural and magnetic properties of Ni–Fe nanowires in the pores of polymer track membranes, *J. Magn. Magn. Mater.*, 2019, vol. 489, art. ID 165415.
18. Doludenko, I.M., Zagorskii, D.L., Frolov, K.V., et al., Nanowires made of FeNi and FeCo alloys: Synthesis, structure, and Mössbauer measurements, *Phys. Solid State*, 2020, vol. 62, no. 9, pp. 1639–1646. https://doi.org/10.1134/S1063783420090061
19. Valizadeh, S., George, J.M., Leisner, P., and Hultman, L., Electrochemical deposition of Co nanowire arrays. Quantitative consideration of concentration profile, *Electrochim. Acta.*, 2001, vol. 47, pp. 865–874.
20. Shin, S., Al-Housseiny, T.T., Kim, B.S., Cho, H.H., and Stone, H.A., The race of nanowires: Morphological instabilities and a control strategy, *Nano Lett.*, 2014, vol. 14, pp. 4395–4399.

Translated by A. Kukharuk

SPELL: OK